

Lane-formation vs. cluster-formation in two dimensional square-shoulder systems: A genetic algorithm approach

Julia Fornleitner^{1,*} and Gerhard Kahl¹

¹*Center for Computational Materials Science and Institut für Theoretische Physik,
Technische Universität Wien, Wiedner Hauptstraße 8-10, A-1040 Wien, Austria*

(Dated: October 31, 2018)

Introducing genetic algorithms as a reliable and efficient tool to find ordered equilibrium structures, we predict minimum energy configurations of the square shoulder system for different values of corona width λ . Varying systematically the pressure for different values of λ we obtain complete sequences of minimum energy configurations which provide a deeper understanding of the system's strategies to arrange particles in an energetically optimized fashion, leading to the competing self-assembly scenarios of cluster-formation vs. lane-formation.

PACS numbers:

The ability of colloidal dispersions to self-organize in a surprisingly large variety of ordered structures markedly distinguishes soft matter from hard (i.e., atomic) materials. The spectrum of ordered particle arrangements encountered in soft matter systems does not only contain low-symmetry, non-close-packed structures, such as bcc, diamond, or the A15 lattices [1, 2, 3, 4, 5]; soft matter particles are able to self-organize in considerably more complex ways, forming thereby micellar and inverse micellar structures [6, 7], cluster phases [8], chain-like or layered arrangements [7, 9, 10, 11, 12, 13], or gyroid phases [14, 15, 16], just to name a few of them.

In the investigation of self-organizing phenomena in soft matter systems, theoreticians have developed reliable tools. On one side efficient and accurate coarse-graining procedures have been developed which, by averaging over the large number of degrees of freedom of the solvent particles [17, 18], lead to effective potentials between the colloidal particles. On the other side there are statistical mechanics based concepts which provide on the basis of these interactions reliable information on the thermodynamic properties that finally lead to the phase diagram of the system at hand. Among those are density functional theory [19], liquid state theories [20], or computer simulations [21].

What is badly missing among the theoreticians' tools is a reliable way of how to *predict* the ordered equilibrium structures for a given system. In hard materials one can safely rely on experience, intuition, or plausible arguments: a set of pre-selected candidate structures is chosen, comprising the usual suspects (such as fcc, bcc, etc.) and at a given state point the lattice with the lowest (free) energy is the stable one. In soft matter, however, the situation is entirely different: as a consequence of the rich wealth of emerging equilibrium structures a conventional approach that is based on a biased pre-selection process is bound to fail. Computer simulations are not very helpful either, since they are time-consuming and

risk to be trapped in local energetic minima due to the rough and complex energy surface.

In this contribution we present an alternative strategy which we believe to be very powerful in the search of equilibrium structures and which does not share the deficiencies of the conventional approaches. We use genetic algorithms (GAs), i.e., optimization strategies, that adopt features of evolutionary processes as key elements to find the optimal solution for a problem [22]. In contrast to the conventional methods, GAs allow for searching basically among *all* lattice structures in a parameter-free and unbiased way. Despite the fact that GAs have been proposed several decades ago [22], their usefulness in problems of condensed matter theory has been acknowledged only in recent years (see, e.g., [23, 24]). In the present contribution we demonstrate the power of this approach for a two-dimensional (2D) system where the particles interact via spherically symmetric square-shoulder potentials. With the help of GAs we identify minimum energy configurations (MECs), or, equivalently the zero-temperature phase diagram.

GAs mimic certain principles and processes known from natural evolution like mutation, mating and 'survival of the fittest' to find the global extremum in the function to optimise. Because of their particular search strategies they are able to investigate large areas in search space and to concentrate at the same time their efforts on the most promising regions. It is in particular this global scope which has made GAs a highly appreciated tool in many fields.

The basic unit of a GA is a so-called *individual*, \mathcal{I} , which represents one possible solution of the problem, encoded in a string of genes. Each gene can take on values out of a chosen alphabet. The encoding of the candidate to the individual is a very delicate task that has major influence on the performance of the GA. A set of individuals is called *generation*.

With these definitions we can sketch the work-flow of a GA: first a starting generation is created at random, whose individuals consist of arbitrary sequences of genes. Each of the individuals \mathcal{I} is assigned a 'fitness-value' through a problem-specific function $f(\mathcal{I})$, assess-

*Electronic address: fornleitner@cmt.tuwien.ac.at

ing the quality of the solution represented by the individual. A higher fitness-value marks a better solution in this evaluation process. According to their fitness, parent individuals are selected for reproduction to generate new individuals by simple operations like recombination and mutation, for which many different methods have been proposed in literature. This circle, i.e., evaluation–selection–recombination–mutation, is iterated until a sufficiently large number of generations has been created. The individual with the absolutely highest fitness value is taken as the final solution. Since GAs do not converge exactly to the global minimum, additional refinement of the proposed solution is required.

In an effort to adapt this general algorithm to our particular problem, we first have to find a suitable encoding of the candidate structures to the individuals. To this end we have utilized two different strategies: **(i)** a simple lattice parametrisation where the lattice vectors and positions of eventual basis particles are translated via the binary alphabet to strings of 0s and 1s; **(ii)** a more refined strategy, which is specially adapted to systems for which cluster phases are to be expected, has been developed: in this ‘cluster-biased’ version the lattice sites are populated by ordered (i.e. regular) dimers or trimers. Hence individuals include additional information describing the orientation and the distance of particles in the cluster. In this way more particles per unit cell can be considered, reducing at the same time the number of parameters. This leads to a considerably enhanced performance of the GA for complex lattices. In addition, for hard-core particles, particular care is in order to prevent the creation of individuals that represent unphysical configurations with overlapping cores.

Working at fixed particle number N , pressure P , and temperature T , we have decided for the standard form of $f(\mathcal{I})$, i.e.,

$$f(\mathcal{I}) = \exp\{-[G(\mathcal{I}) - G_0]/G_0\} \quad . \quad (1)$$

At $T = 0$, the Gibbs free energy, G , reduces to $G = U + PV$, V being the volume. G_0 stands for the Gibbs free energy of a reference structure. For further conceptual and numerical details concerning the GA we refer to [25, 26].

The interaction potential of the square-shoulder system consists of an impenetrable core of diameter σ with an adjacent step-shaped, repulsive corona (with range $\lambda\sigma$), i.e.,

$$\Phi(r) = \begin{cases} \infty & r \leq \sigma \\ \epsilon & \sigma < r < \lambda\sigma \end{cases} \quad , \quad (2)$$

ϵ being the height of the shoulder. The search for MECs for this particular system represents undoubtedly the most stringent test for the GA: with its flat plateau and as sharp a cutoff as possible the MECs can be easily classified by the number of overlapping coronas which makes the potential a quintessential [2] test system. The fact that we restrict ourselves to a 2D system does not represent a limitation at all. On the contrary, the particle

arrangements can be visualized in a very convenient way that makes it much easier to understand the sequence of MECs as the pressure is increased. Objections that the system is oversimplified and only of academic interest can easily be refuted: there exist a number of realistic soft systems with a core-corona-architecture that can be described using a square-shoulder interaction [13]. Among these are, for instance, colloidal particles with block-copolymers grafted to their surface where self-consistent field calculations lead to effective interactions that closely resemble $\Phi(r)$ given in (2) [27].

The search for MECs for the square-shoulder potential has been pioneered by Jagla [9, 10] and was carried on in later work by Malescio and Pellicane [12, 13] using Monte Carlo simulations and geometrical considerations. Further theoretical work on this system was presented in [7]. The results are indeed remarkable: a large variety of MECs has been identified where – despite the radial symmetry of $\Phi(r)$ – particles often arrange in asymmetric structures, forming thereby lanes or ring-like structures. However, the authors of above mentioned studies raise doubts themselves that their set of MECs might not be complete. Introducing GAs as a novel technique to this particular problem, we will present in the following sequences of MECs that show a considerably larger variety than the ones identified up to now and which can easily be understood via energetic arguments. Although we cannot provide a rigorous proof there is evidence that these sequences are complete.

Our results offer – depending on the range of the shoulder λ – a deeper insight that the square-shoulder system develops different strategies to form MECs. Among the systems we have investigated we present in the following results for three different values for λ , corresponding to a small ($\lambda = 1.5$), an intermediate ($\lambda = 4.5$), and a large shoulder range ($\lambda = 10$). Standard reduced units are used: $P^* = P\sigma^2/\epsilon$, $U^* = U/(N\epsilon)$ and $G^* = G/(N\epsilon) = U^* + P^*/(\eta\sigma^2)$, $\eta = N/V$ being the number density.

We start with $\lambda = 1.5$ and show in Fig. 1 the MECs proposed by the GA, while Fig. 2 displays the corresponding thermodynamic properties G^* and U^* as functions of P^* . At very low pressure, particles populate an ideal hexagonal lattice, thus avoiding overlapping coronas. Upon compression, the system must pay in some form tribute to the reduced space in terms of an energy penalty, i.e. via a first overlap of shoulders. Obviously, for this λ -value, the formation of lanes is energetically the best solution. Along these lanes, particles are in direct contact (and, consequently have overlapping coronas), forming a one-dimensional close-packed arrangement. Parallel lanes, however, try to avoid corona overlap and the shoulder width λ serves as a spacer (see magnified view). As the pressure is further increased, new strategies are required. While particles still prefer alignment along lanes their internal arrangement is modified: rather than forming straight lines, the lanes are zig-zag shaped due to energetic reasons, which is a compromise between

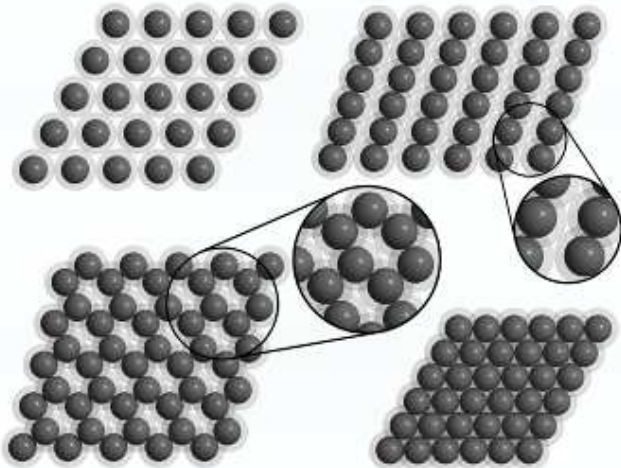


FIG. 1: MECs for the square-shoulder system of shoulder range $\lambda = 1.5$. Configurations correspond (from left to right and from top to bottom) to pressure values indicated in Fig. 2 by vertical arrows.

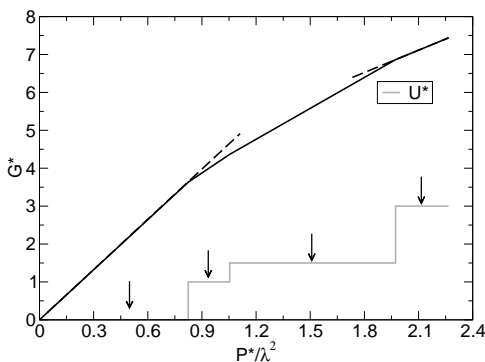


FIG. 2: G^* (black line) and U^* (grey line) as functions of P^*/λ^3 for the square-shoulder system with $\lambda = 1.5$. Vertical arrows indicate MECs depicted in Fig. 1. Broken lines represent limiting cases of MECs (see text).

the reduced available space and the imminent energetic penalty due to additional corona overlaps. Neighbouring lanes are arranged in such a way, that each particle is now in direct contact with three other ones. Alternatively, the staggered lanes can also be viewed as a ring-like structure: six particles form elongated rings where λ serves again as a spacer, fixing the width of the cage. In the end, further compression causes the system to collapse into the close-packed hexagonal structure where each particle is in direct contact with six neighbours.

The functional form of G^* and U^* can nicely be understood via the following, general thermodynamic considerations (cf. Fig. 2): For a given particle configuration, characterized by the number of overlapping coronas, U^* is constant; thus $G^* = U^* + P^*/(\eta\sigma^2)$ is a straight line as a function of P^* with slope $1/\eta$. Two limiting cases

(indicated as broken lines in Fig. 2 and characterized by slopes $1/\eta_{\min}$ and $1/\eta_{\max}$) can easily be identified: an arrangement where disks of diameter λ form a close-packed structure (with η_{\min} and $U^* = 0$) and the hexagonal lattice where the particles' hard cores form a close-packed structure (with η_{\max} and $U^* = U^*_{\max} = 3$). All other MECs identified by the GA are located on lines of slope $1/\eta$, with $1/\eta_{\max} \leq 1/\eta \leq 1/\eta_{\min}$, and obviously have lower G^* -values. Thus $G^* = G^*(P^*)$ becomes a sequence of intersecting straight lines, representing a considerable help in analysing the data. Cross-over points between two competing structures where GAs tend to have convergence problems [25] can be determined *exactly* as the intersection of two straight lines. The energy levels U^* (also depicted in Fig. 2) that characterize the MECs are of course rational numbers, i.e., number of overlapping coronas divided by the number of particles per unit cell. Finally, all calculations have been performed on rather fine pressure grids ($\Delta P^* \sim 0.2$) so we are confident that the presented sequences of MECs are complete.

As we proceed to $\lambda = 4.5$ the systems develops completely different strategies to form MECs as the pressure is increased; they are depicted in Fig. 3, while Fig. 4 displays the thermodynamic properties. The hexagonal pattern imposed by the non-overlapping coronas (observed at extremely low pressure-values and not displayed here) is soon superseded by a novel strategy, namely cluster formation. At low pressure, dimers are formed which populate the sites of a distorted hexagonal lattice. Upon further compression, these aggregates become larger until they reach the size of six particles. The degree of distortion of the underlying hexagonal lattice is imposed by the shape of the clusters: therefore, the trimers, which have nearly circular shape, sit on a nearly perfect hexagonal lattice, while for elongated hexamers the structure is strongly distorted. As the system is further compressed, formation of clusters is obviously energetically less attractive and lane-formation sets in. With increasing pressure the structure of the MECs becomes more complex. In the beginning each lane is built up by a linear sequence of dimers and thus closely resembles the first lane-scenario observed for $\lambda = 1.5$. At higher pressure-values, however, the system forms parallel lanes which are now built up by larger clusters. The increasing complexity of this inner structure makes simple energetic explanations in terms of overlapping coronas impossible. However, the grey shades in Fig. 3 give evidence that the formation of clustered lanes is an efficient strategy to avoid an overlap between neighbouring lanes, which represents a considerably higher energy penalty. The tendency to form parallel lanes is maintained until the system finally collapses into the close-packed hexagonal structure. The considerably richer wealth of MECs encountered for $\lambda = 4.5$ is reflected by the large number of energy levels in the plot U^* vs. P^* and the number of intersecting straight line segments in the diagram of G^* vs. P^* .

Finally, for $\lambda = 10$, the strategies of the system to form MECs seem at first sight similar to the previous case:

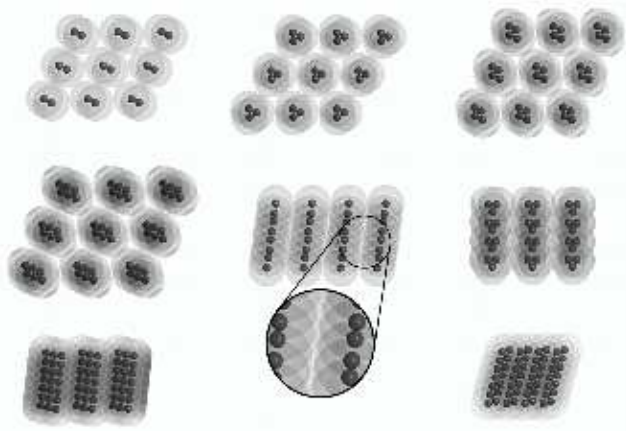


FIG. 3: MECs for the square-shoulder system of shoulder range $\lambda = 4.5$. Configurations correspond (from left to right and from top to bottom) to pressure values indicated in Fig. 4 by vertical arrows.

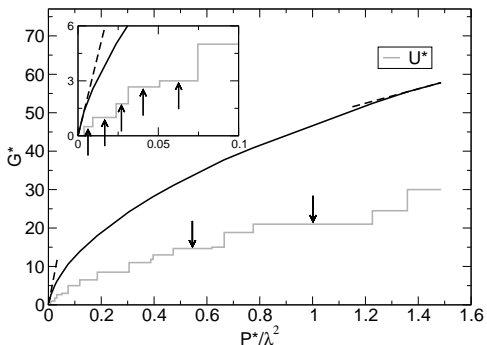


FIG. 4: G^* (black line) and U^* (grey line) as functions of P^*/λ^3 for the square-shoulder system with $\lambda = 4.5$. Vertical arrows indicate MECs depicted in Fig. 3. Broken lines represent limiting cases of MECs (see text).

again, the system prefers formation of clusters at low pressure, which are located on slightly distorted hexagonal lattices. However, we observe that inside a cluster the cores of the particles are sometimes arranged in a disordered fashion, while for $\lambda = 4.5$ only clusters with an ordered internal particle arrangement occur. The strategy is obviously the following: once λ is sufficiently large so that cluster formation is supported, the system tries to arrange particles so that the shape of the cluster becomes as circular as possible. This in turn guarantees that the underlying structure is close to the energetically most favourable hexagonal lattice. For $\lambda = 4.5$, where the core region still represents a considerable fraction of the particle diameter, the system has to proceed rather carefully to fulfill this requirement, leading to the ordered arrangements of the cores. For $\lambda = 10$, however, the core region is nearly negligible with respect to the core width. Now both regular and irregular particle ar-

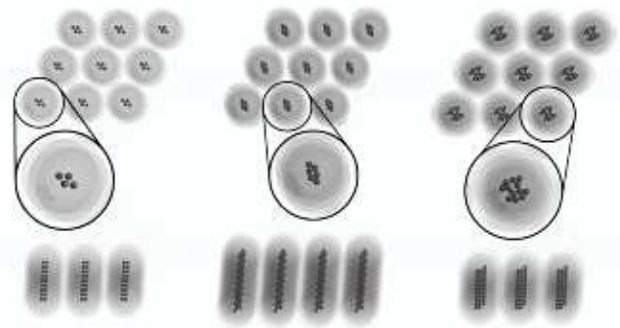


FIG. 5: MECs for the square-shoulder system of shoulder range $\lambda = 10$. Configurations correspond (from left to right and from top to bottom) to pressure values indicated in Fig. 6 by vertical arrows.

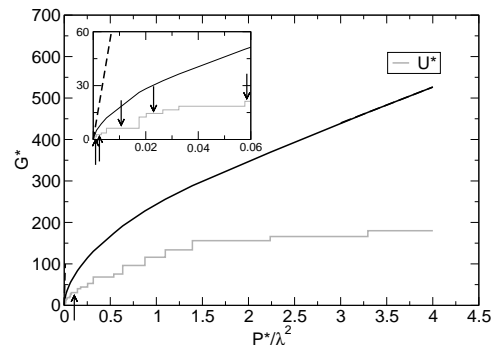


FIG. 6: G^* (black line) and U^* (grey line) as functions of P^*/λ^3 for the square-shoulder system with $\lambda = 10$. Vertical arrows indicate MECs depicted in Fig. 5. Broken lines represent limiting cases of MECs (see text).

rangements inside the core can lead to circular-shaped clusters of the same size, having practically the same G -value. Again, at higher pressure values lanes with an increasingly complex inner structure are formed. Some of them (for example, the last one displayed in Fig. 5) might be comparable to the Bernal spirals observed experimentally in three dimensional colloidal systems [28]. Lane formation persists until the system finally collapses into the close-packed hexagonal structure. If the square-shoulder particles still represent a reasonable model for macromolecules at such high pressure values is questionable.

Let us come back to the disordered clusters. If we extrapolate these results to even larger values of λ – or, equivalently, to a vanishing core – and briefly switch to three dimensions, we arrive at another soft matter model system that has been studied in detail in literature: the penetrable sphere model (PSM) [29]. Among the remarkable, well-documented features of this system is its ability to form cluster phases: at sufficiently high densities clusters of overlapping particles populate the lattice sites of

a regular fcc lattice. Detailed simulations of a closely related system that also shows clustering [8] have revealed that the internal structure of the clusters is completely random. These observations are consistent with our results in the sense, that an increasing corona width (or, equivalently, a vanishing core) favours formation of disordered clusters of particles, which in turn populate sites of regular lattices. Obviously first precursors of this phenomenon occur at $\lambda = 10$ [30].

Our results provide an explanation for the system's strategy to form MECs: if λ is small, formation of larger clusters is prohibited due to geometric reasons, hence particles arrange in lanes of variable shape or in connected structures. However, as soon as the range of the corona is sufficiently large, the formation of clusters sets in and they dominate the low-pressure regime. Depending on the corona range, the particles group in ordered or disordered clusters, keeping the cluster's shape as disk-like as and the underlying structure as close to the ideal hexagonal lattice as possible. For systems that exhibit clustering, lane formation sets in at higher pressure values. The lanes themselves are built up by clusters, so one is led to interpret the crossover to the lane regime as a

structural change of the cluster crystal.

The results of our investigations are, on one side, of rather basic relevance. The simple form of the potential allows to understand the full sequence of MECs on an energetic level as the pressure is increased and thus provides deeper insight under which conditions the system prefers to form either lanes or clusters. But also from a more applied point of view, these results are of relevance. Having established GAs as a suitable and reliable tool for finding ordered equilibrium structures, the strategies of self-assembly of systems with a substantially more complex effective interparticle interaction can be better understood. Such knowledge is certainly of relevance in technological applications, such as nanolithography or nanoelectricity.

Acknowledgements The authors are indebted to Dieter Gottwald and Gernot J. Pauschenwein (both Wien), Christos N. Likos (Düsseldorf), and Primoz Zihlerl (Ljubljana) for stimulating discussions. Financial support by the Austrian Science Foundation (FWF) under Proj. Nos. P15758-N08 and P19890-N16 is gratefully acknowledged.

-
- [1] Zihlerl, P.; Kamien, R. *Phys. Rev. Lett.* **2000**, *85*, 3528.
 [2] Zihlerl, P.; Kamien, R. *J. Phys. Chem. B* **2001**, *105*, 10147.
 [3] Watzlawek, M.; Likos, C.; Löwen, H. *Phys. Rev. Lett.* **1999**, *82*, 5289.
 [4] Gottwald, D.; Likos, C.; Kahl, G.; Löwen, H. *Phys. Rev. Lett.* **2004**, *92*, 068301.
 [5] Gottwald, D.; Likos, C.; Kahl, G.; Löwen, H. *J. Chem. Phys.* **2005**, *122*, 074903.
 [6] Pierleoni, C.; Addison, C.; Hansen, J.-P.; Krakoviack, V. *Phys. Rev. Lett.* **2006**, *96*, 128302–1.
 [7] Glaser, M.; Grason, G.; Kamien, R.; Košmrlj, A.; Santangelo, C.; Zihlerl, P. *Europhys. Lett.* **2007**, *78*, 46004.
 [8] Mladek, B.; Gottwald, D.; Kahl, G.; Neumann, M.; Likos, C. *Phys. Rev. Lett.* **2006**, *96*, 045701.
 [9] Jagla, E. *Phys. Rev. E* **1998**, *58*, 1478.
 [10] Jagla, E. *J. Chem. Phys.* **1999**, *110*, 451.
 [11] Camp, P. *Phys. Rev. E* **2003**, *68*, 061506.
 [12] Malescio, G.; Pellicane, G. *Nat. Materials* **2003**, *2*, 97.
 [13] Malescio, G.; Pellicane, G. *Phys. Rev. E* **2004**, *70*, 021202.
 [14] Hajduk, D.; Harper, P.; Gruner, S.; Honeker, C.; Kim, G.; Thomas, E.; Fetters, L. *Macromolecules* **1994**, *27*, 4063.
 [15] Matsen, W. *J. Chem. Phys.* **1998**, *108*, 785.
 [16] Ullal, C.; Maldovan, M.; Thomas, E.; Chen, G.; Han, Y.; Yang, S. *Phys. Rev. Lett.* **2004**, *84*, 5434.
 [17] Likos, C. *Phys. Rep.* **2001**, *348*, 267.
 [18] Ballauff, M.; Likos, C. *Angew. Chemie Intl. English Ed.* **2004**, *43*, 2998.
 [19] Evans, R.; Marcel Dekker, New York, 1992; chapter 3, pages 85–175.
 [20] Hansen, J.-P.; McDonald, I. *Theory of Simple Liquids*; Elsevier, Amsterdam, 3rd ed., 2006.
 [21] Frenkel, D.; Smit, B. *Understanding Molecular Simulations*; Academic Press, London, 2nd ed., 2002.
 [22] Holland, J. *Adaption in Natural and Artificial Systems*; The University of Michigan Press, Ann Arbor, 1975.
 [23] Oganov, A.; Glass, C. *J. Chem. Phys.* **2006**, *124*, 244704.
 [24] Siepmann, P.; Martin, C.; Vancea, I.; Moriarty, P.; Krasnogor, N. *Nano Letters* **2007**, *7*, 1985–1990.
 [25] Gottwald, D.; Kahl, G.; Likos, C. *J. Chem. Phys.* **2005**, *122*, 204503–1.
 [26] Fornleitner, J.; Kahl, G. *to be published*
 [27] Norizoe, Y.; Kawakatsu, T. *Europhys. Lett.* **2005**, *72*, 583.
 [28] Campbell, A.; Anderson, V.; van Duijneveldt, J.; Bartlett, P. *Phys. Rev. Lett.* **2005**, *94*, 208301.
 [29] Likos, C. N.; Watzlawek, M.; Löwen, H. *Phys. Rev. E* **1998**, *58*, 3135–3144.
 [30] Likos, C. N.; Mladek, B. M.; Gottwald, G.; Kahl, G. *J. Chem. Phys.* **2007**, *126*, 224502.